JOC Featured Article

pubs.acs.org/joc

Self-Assembled Boronic Ester Cavitand Capsule as a Photosensitizer and a Guard Nanocontainer against Photochemical Reactions of 2,6-Diacetoxyanthracene

Naoki Nishimura and Kenji Kobayashi*

Department of Chemistry, Faculty of Science, Shizuoka University, 836 Ohya, Suruga-ku, Shizuoka 422-8529, Japan

skkobay@ipc.shizuoka.ac.jp

Received July 1, 2010

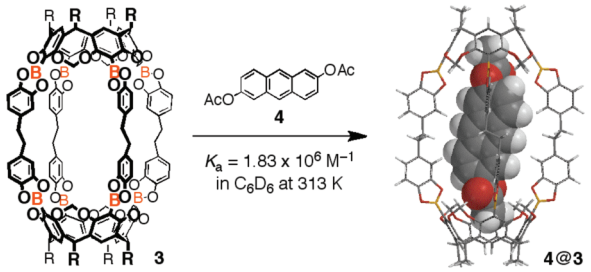

The optical properties of 2,6-diacetoxyanthracene **4** encapsulated in the self-assembled boronic ester cavitand capsule **3** in C_6H_6 are described. Upon excitation at 285 nm, the encapsulated **4** showed strong fluorescence emission as a result of the energy transfer from the excited **3** to the encapsulated **4**, while **4** alone in C_6H_6 exhibited very weak emission. Upon photoirradiation at 365 nm, the encapsulated **4** also showed strong fluorescence emission and remained almost intact, whereas **4** alone in C_6H_6 gradually underwent photodimerization and photooxygenation to afford photodimers **5** and **5′** and 9,10-anthraquinone **6** via 9,10-endoperoxide **7**, respectively. Thus, the capsule **3** serves as a photosensitizer for the encapsulated **4** as well as a guard nanocontainer to protect against the photochemical reactions of **4**.

Introduction

It is well-known that anthracene and its derivatives react under photoirradiation at 360−370 nm to afford [4π+4π] photodimerization products and [4π+2π] photooxygenation products (9,10-endoperoxides) and that these products return to the monomer state under UV irradiation below 270 nm in the former case and by the transfer of thermal energy in both cases.[1] These reversible switching properties of anthracene derivatives in response to external photochemical and thermal stimuli have been applied to supramolecular architectures.[2] Anthracene and its derivatives are also useful building blocks for optoelectronics, such as organic electroluminescent devices,[3,4] and for organic semiconductors such as organic field-effect transistors[5] and organic photoconductors.[6] However, photodimerization and photooxygenation of anthracene derivatives are disadvantageous for uses related to optoelectronics.

Self-assembled molecular capsules have potential as reaction nanovessels,[7] as well as nanocontainers for the stabilization

(1) (a) Becker, H.-D. *Chem. Rev.* **1993**, *93*, 145–172. (b) Bouas-Laurent, H.; Castellan, A.; Desvergne, J.-P.; Lapouyade, R. *Chem. Soc. Rev.* **2000**, *29*, 43–55. (c) Bouas-Laurent, H.; Castellan, A.; Desvergne, J.-P.; Lapouyade, R. *Chem. Soc. Rev.* **2001**, *30*, 248–263. (d) Aubry, J.-M.; Pierlot, C.; Rigaudy, J.; Schmidt, R. *Acc. Chem. Res.* **2003**, *36*, 668–675.

(2) (a) Molard, Y.; Bassani, D. M.; Desvergne, J.-P.; Horton, P. N.; Hursthouse, M. B.; Tucker, J. H. R. *Angew. Chem., Int. Ed.* **2005**, *44*, 1072–1075. (b) Al-Kaysi, R. O.; Müller, A. M.; Bardeen, C. J. *J. Am. Chem. Soc.* **2006**, *128*, 15938–15939. (c) Schäfer, C.; Eckel, R.; Ros, R.; Mattay, J.; Anselmetti, D. *J. Am. Chem. Soc.* **2007**, *129*, 1488–1489. (d) Zehm, D.; Fudickar, W.; Linker, T. *Angew. Chem., Int. Ed.* **2007**, *46*, 7689–7692. (e) Al-Kaysi, R. O.; Bardeen, C. J. *Adv. Mater.* **2007**, *19*, 1276–1280. (f) Garcia-Garibay, M. A *Angew. Chem., Int. Ed.* **2007**, *46*, 8945–8947. (g) Hirose, K.; Ishibashi, K.; Shiba, Y.; Doi, Y.; Tobe, Y. *Chem.—Eur. J.* **2008**, *14*, 5803–5811 and references cited therein

(3) Hung, L. S.; Chen, C. H. *Mater. Sci. Eng., R* **2002**, *39*, 143–222.

(4) Iida, A.; Yamaguchi, S. *Chem. Commun.* **2009**, 3002–3004 and references cited therein.

(5) (a) Ito, K.; Suzuki, T.; Sakamoto, Y.; Kubota, D.; Inoue, Y.; Sato, F.; Tokito, S. *Angew. Chem., Int. Ed.* **2003**, *42*, 1159–1162. (b) Meng, H.; Sun, F.; Goldfinger, M. B.; Gao, F.; Londono, D. J.; Marshall, W. J.; Blackman, G. S.; Dobbs, K. D.; Keys, D. E. *J. Am. Chem. Soc.* **2006**, *128*, 9304–9305. (c) Zhao, Q.; Kim, T. H.; Park, J. W.; Kim, S. O.; Jung, S. O.; Kim, J. W.; Ahn, T.; Kim, Y.-H.; Yi, M. H.; Kwon, S.-K. *Adv. Mater.* **2008**, *20*, 4868–4872.

(6) Marrocchi, A.; Silvestri, F.; Seri, M.; Facchetti, A.; Taticchia, A.; Marks, T. J. *Chem. Commun.* **2009**, 1380–1382.

DOI: 10.1021/jo101255g Published on Web 08/17/2010

SCHEME 1. Encapsulation of 2,6-Diacetoxyanthracene 4 in Boronic Ester Cavitand Capsule 3 Self-Assembled by 1 and 2

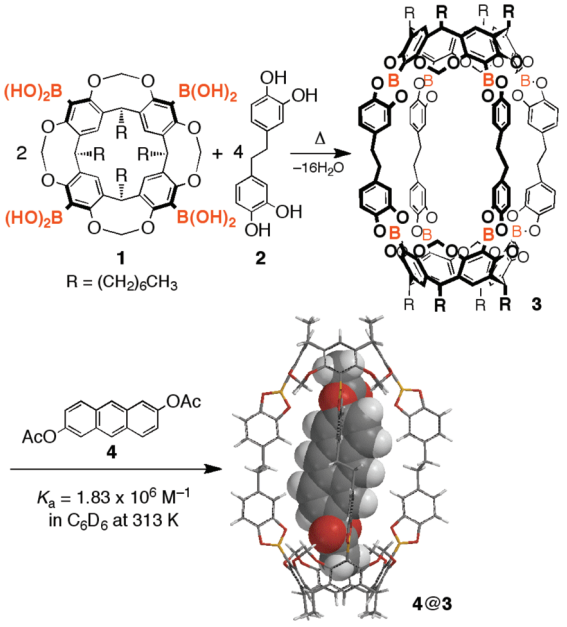

of reactive intermediates,[7,8] and for the control of photochemical properties and reactions of encapsulated guests.[9,10] Recently, we reported on the encapsulation of 2,6-diacetoxyanthracene **4** in the self-assembled boronic ester cavitand capsule **3** (Scheme 1).[11] The latter is synthesized by the dynamic boronic ester formation of cavitand tetraboronic acid **1** with the bis-catechol linker **2**.[11] We now describe the use of the capsule **3** as a photosensitizer for the encapsulated **4**,[12] as well as a guard nanocontainer to protect against the photochemical reactions of **4** (Figure 1).[13] The guest-encapsulating capsule **4**@**3** serves as a photostable luminescence material.

Results and Discussion

UV−vis Absorption and Fluorescence Emission Spectra of 4@3. The self-assembled boronic ester cavitand capsule **3** encapsulates one molecule of 2,6-diacetoxyanthracene **4** with an association constant (K_a) of 1.83×10^6 M^{-1} in C_6D_6 at 313 K.[11b] The UV−vis absorption and fluorescence emission spectra of guest-free **3**, free-**4**, and the guest-encapsulating capsule **4**@**3** were measured at a concentration of 1.0×10^{-5} M in C_6H_6 at 296 K. Under these conditions, **3** maintains 100% encapsulation of **4** upon addition of 1 equiv of **4**, and **4**@**3** does not release **4**. The UV−vis absorption spectra of free-**3**, free-**4**, and **4**@**3** showed the absorption maxima (λ_{max}(abs)) at 277 nm for free-**3**; at 349, 361, and 382 nm for free-**4**; and at 277, 348, 361, and 382 nm for **4**@**3** (Figure 2 and Table 1).[14,15] The λ_{max}(abs) of **4** encapsulated in **3** was almost the same as that of free-**4** in C_6H_6.

The fluorescence emission spectra and spectral data of free-**3**, free-**4**, and **4**@**3** are shown in Figure 3 and Table 2.[15] Upon excitation at 360 nm, free-**4** and **4**@**3** showed fluorescence emission maxima (λ_{max}(em)) at 394 nm (peak A) and 415 nm (peak B) for free-**4** and at 393 nm (peak A) and 413 nm (peak B) for **4**@**3**, whereas free-**3** alone was not emissive (Figure 3a). The λ_{max}(em) of **4** encapsulated in **3** was slightly blue-shifted by 1−2 nm relative to that of free-**4**, and the fluorescence emission intensities of **4**@**3** decreased by 8% relative to the intensities of free-**4**. In marked contrast, *upon excitation at 285 nm*, the fluorescence emission intensities of peaks A and B of **4**@**3** increased by 15% relative to those upon excitation at 360 nm, whereas the fluorescence emission intensities of free-**4** upon excitation at 285 nm decreased by 96% relative to those upon excitation at 360 nm (Figure 3b vs 3a). As a result, upon excitation at 285 nm the fluorescence emission intensities of peaks A and B of **4**@**3** were 30 times stronger than those of free-**4** in C_6H_6 (Figure 3b). Upon excitation at 285 nm the λ_{max}(em) of **4**@**3** also appeared at 341 nm (peak C), in addition to peak A and peak B, because the free-**3** alone showed the fluorescence emission peak C upon excitation at 285 nm (Figure 3b), wherein the fluorescence emission intensity of free-**3** was six times stronger than that of **4**@**3**.

Capsule 3 as a Photosensitizer for the Encapsulated Guest 4. The fluorescence excitation spectra and spectral data of free-**4** and **4**@**3** upon fluorescence emission at 410 nm in C_6H_6 at 296 K are shown in Figure 4 and Table 3, respectively. For free-**4**, the fluorescence emission at 410 nm mainly arises from the excitation maxima (λ_{max}(ex)) at 348, 359, and 381 nm. For **4**@**3**, the fluorescence emission at 410 nm mainly arises from λ_{max}(ex) at 285 nm, as well as at 348, 360, and 381 nm. The fluorescence excitation spectral pattern of **4**@**3** upon fluorescence emission at 410 nm is similar to the UV−vis absorption spectral pattern of **4**@**3**. These results clearly indicate that the strong fluorescence emission of **4**@**3** upon excitation at 285 nm shown in Figure 3b is caused by the

(7) (a) Rebek, J., Jr. *Angew. Chem., Int. Ed.* **2005**, *44*, 2068–2078. (b) Yoshizawa, M.; Klosterman, J. K.; Fujita, M. *Angew. Chem., Int. Ed.* **2009**, *48*, 3418–3438. (c) Pluth, M. D.; Bergman, R. G.; Raymond, K. N. *Acc. Chem. Res.* **2009**, *42*, 1650–1659.

(8) For covalent-bound molecular capsules for stabilization of reactive chemical species, see: (a) Warmuth, R.; Yoon, J. *Acc. Chem. Res.* **2001**, *34*, 95–105. (b) Warmuth, R.; Makowiec, S. *J. Am. Chem. Soc.* **2007**, *129*, 1233–1241 and references cited therein

(9) (a) Yoshizawa, M.; Takeyama, Y.; Okano, T.; Fujita, M. *J. Am. Chem. Soc.* **2003**, *125*, 3243–3247. (b) Kaanumalle, L. S.; Gibb, C. L. D.; Gibb, B. C.; Ramamurthy, V. *J. Am. Chem. Soc.* **2005**, *127*, 3674–3675. (c) Kaanumalle, L. S.; Ramamurthy, V. *Chem. Commun.* **2007**, 1062–1064. (d) Parthasarathy, A.; Kaanumalle, L. S.; Ramamurthy, V. *Org. Lett.* **2007**, *9*, 5059–5062. (e) Gibb, C. L. D.; Sundaresan, A. K.; Ramamurthy, V.; Gibb, B. C. *J. Am. Chem. Soc.* **2008**, *130*, 4069–4080. (f) Ams, M. R.; Ajami, D.; Craig, S. L.; Yang, J.-S.; Rebek, J., Jr. *J. Am. Chem. Soc.* **2009**, *131*, 13190–13191.

(10) For control of product selectivity in organic phototransformation in supramolecular systems, see: Tung, C.-H.; Wu, L.-Z.; Zhang, L.-P.; Chen, B. *Acc. Chem. Res.* **2003**, *36*, 39–47.

(11) (a) Nishimura, N.; Kobayashi, K. *Angew. Chem., Int. Ed.* **2008**, *47*, 6255–6258. (b) Nishimura, N.; Yoza, K.; Kobayashi, K. *J. Am. Chem. Soc.* **2010**, *132*, 777–790.

(12) For enhancement in the fluorescence emission of chromophores by energy transfer in supramolecular systems, see: (a) Slone, R. V.; Hupp, J. T. *Inorg. Chem.* **1997**, *36*, 5422–5423. (b) Choi, M.-S.; Yamazaki, T.; Yamazaki, I.; Aida, T. *Angew. Chem., Int. Ed.* **2004**, *43*, 150–158. (c) Inagaki, S.; Ohtani, O.; Goto, Y.; Okamoto, K.; Ikai, M.; Yamanaka, K.; Tani, T.; Okada, T. *Angew. Chem., Int. Ed.* **2009**, *48*, 4042–4046.

(13) For stabilization of photoreactive organic dyes by rotaxane encapsulations, see: (a) Frampton, M. J.; Anderson, H. L. *Angew. Chem., Int. Ed.* **2007**, *46*, 1028–1064. (b) Yau, C. M. S.; Pascu, S. I.; Odom, S. A.; Warren, J. E.; Klotz, E. J. F.; Frampton, M. J.; Williams, C. C.; Coropceanu, V.; Kuimova, M. K.; Phillips, D.; Barlow, S.; Brédas, J.-L.; Marder, S. R.; Millar, V.; Anderson, H. L. *Chem. Commun.* **2008**, 2897–2899.

(14) The λ_{max}(abs) of **4** at around 255 nm is canceled by that of benzene as a reference solvent.

(15) For UV−vis absorption and fluorescence spectra of **1**, **2**, cavitand without boryl groups **9** as a reference of **1**, and *p*-tolylboronic acid bis(catechol)ethane diester **10** as a reference of **3**, see Figures S1 and S2, Supporting Information.

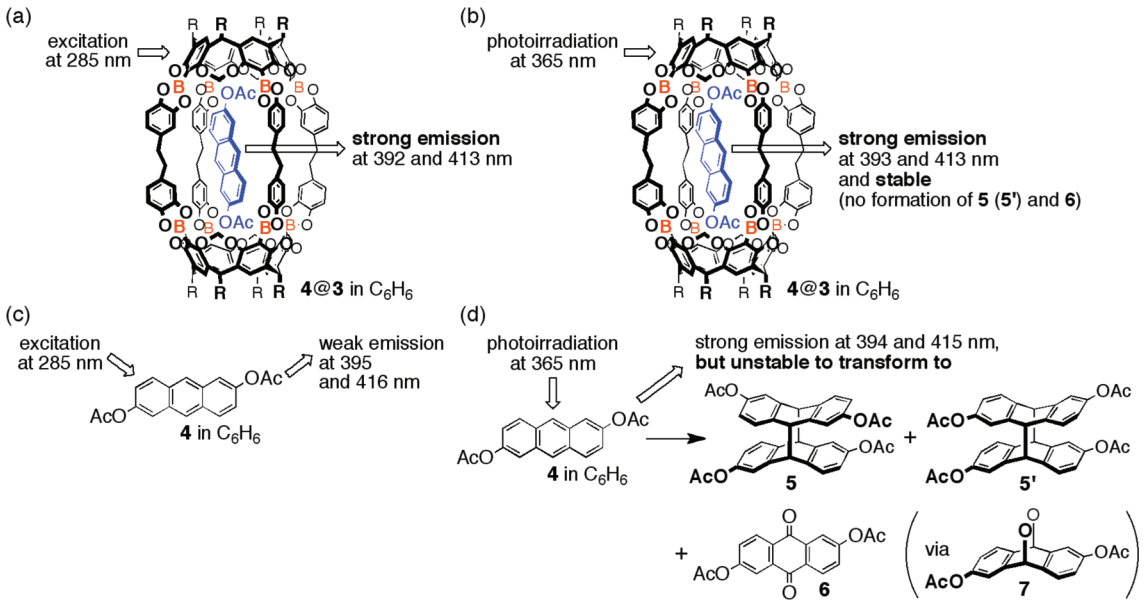

FIGURE 1. Use of capsule **3** as (a) a photosensitizer for the encapsulated **4** and (b) a guard nanocontainer to protect against the photochemical reactions of **4**. (c, d) Photochemical properties of **4** alone.

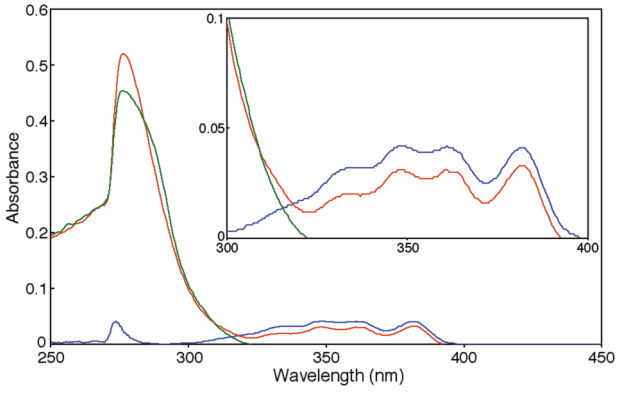

FIGURE 2. UV−vis absorption spectra of free-**3** (green line), free-**4** (blue line), and **4**@**3** (red line) (1.0×10^{-5} M in C_6H_6 at 296 K).

TABLE 1. UV−vis Absorption Spectral Data of Free-3, Free-4, and 4@3 in C_6H_6 (1.0×10^{-5} M) at 296 K

free-**3**		free-**4**		**4**@**3**	
λ_{max}(abs) (nm)	abs	λ_{max}(abs) (nm)	abs	λ_{max}(abs) (nm)	abs
277	0.454	274	0.041	277	0.521
		349	0.042	348	0.031
		361	0.042	361	0.031
		382	0.041	382	0.033

energy transfer from the excited capsule **3** to the encapsulated **4**; i.e., the capsule **3** serves as a photosensitizer for the encapsulated **4**.[12]

To further confirm that the capsule **3** serves as a photosensitizer for the encapsulated **4**, competitive encapsulation experiments between **4** and other guests were carried out (Scheme 2). It is known that 2,6-diacetoxy-9,10-anthraquinone **6** and 4,4′-diacetoxybiphenyl **8** are good guests for **3** ($K_a = 4.25 \times 10^6$ and 1.26×10^6 M^{-1}, respectively, in C_6D_6 at 313 K).[11b] Thus, **6** and **8** are good competitors with respect to **4** ($K_a = 1.83 \times 10^6$ M^{-1}) for the encapsulation in **3**. Figure S4

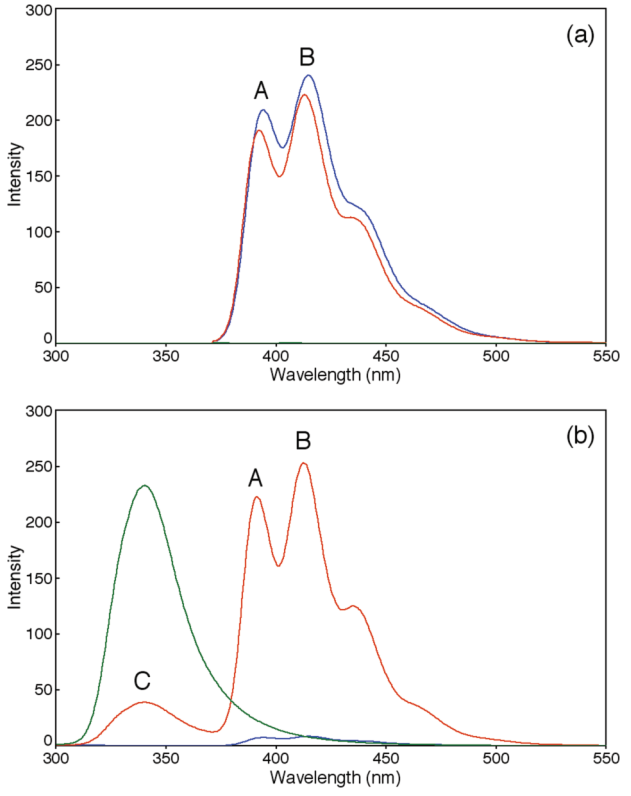

FIGURE 3. Fluorescence emission spectra of free-**3** (green line), free-**4** (blue line), and **4**@**3** (red line) upon excitation at (a) 360 nm and (b) 285 nm (1.0×10^{-5} M in C_6H_6 at 296 K).

(Supporting Information) shows the fluorescence emission spectra of free-**3**, free-**6**, free-**8**, **6**@**3**, and **8**@**3** (1.0×10^{-5} M in C_6H_6 at 296 K) upon excitation at 285 nm. Free-**6** and free-**8** alone were almost nonemissive. Upon excitation at 285 nm, the fluorescence emission intensity at 341 nm of **6**@**3** decreased by 83% relative to that of free-**3**, indicating that the

TABLE 2. Fluorescence Emission Spectral Data of Free-3, Free-4, and 4@3 in C_6H_6 (1.0×10^{-5} M) at 296 K upon Excitation at 360 nm and at 285 nm

	free-**3**		free-**4**		**4@3**	
λ (ex) (nm)	λ_{max}(em) (nm)	int	λ_{max}(em) (nm)	int	λ_{max}(em) (nm)	int
360			394	209.5	393	191.0
			415	240.5	413	223.1
285	341	233.1			341	39.0
			395	7.4	392	222.6
			416	8.5	413	253.1

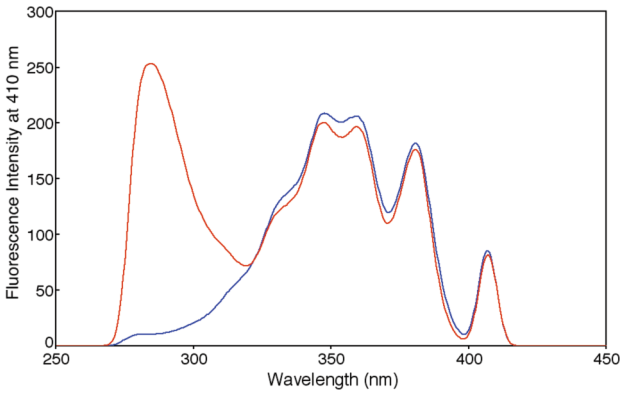

FIGURE 4. Fluorescence excitation spectra of free-**4** (blue line) and **4@3** (red line) upon fluorescence emission at 410 nm (1.0×10^{-5} M in C_6H_6 at 296 K).

TABLE 3. Fluorescence Excitation Spectral Data of Free-4 and 4@3 in C_6H_6 (1.0×10^{-5} M) at 296 K upon Fluorescence Emission at 410 nm

free-**4**		**4@3**	
λ (ex) (nm)	int	λ (ex) (nm)	int
		285	253.3
348	208.6	348	200.4
359	206.2	360	196.9
381	181.7	381	176.3

SCHEME 2. Competitive Encapsulation between 4 and Other Guests upon Encapsulation in 3

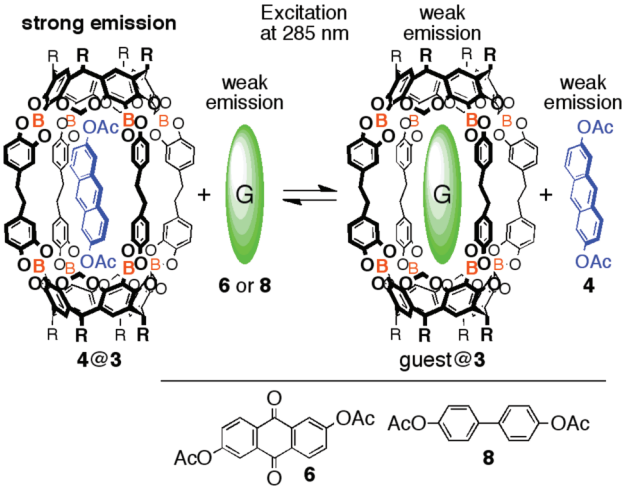

fluorescence quenching of **3** is probably due to energy transfer from the excited **3** to the encapsulated **6**. On the other hand, the fluorescence emission intensity at 341 nm of **8**@**3** increased slightly relative to that of free-**3**. The fluorescence emission spectra and spectral data of a 1:1:1 mixture of **3**, **4**, and **6** or **8** (1.0×10^{-5} M each) in C_6H_6 at 296 K upon excitation at 285 nm are shown in Figure 5a and Table S1 (Supporting Information), respectively. Their fluorescence excitation spectra and spectral data upon fluorescence emission at 410 nm are also shown in Figure 5b and Table S2 (Supporting Information), respectively. Upon excitation at 285 nm, the fluorescence emission intensity at 413 nm from **4** in a 1:1:1 mixture of **3**, **4**, and **6** decreased by 57% relative to that of **4@3** (Figure 5a). In contrast, the fluorescence emission intensity at 413 nm from **4** in a 1:1:1 mixture of **3**, **4**, and **8** decreased by only 19% relative to that of **4@3**. This trend is related to the order of the K_a values of the capsule **3** with guests **8** < **4** < **6**. These results clearly indicate that the fluorescence emission from **4** in a 1:1 mixture of **3** and **4** upon excitation at 285 nm occurs as a result of the intramolecular energy transfer from the excited **3** to the encapsulated **4**.

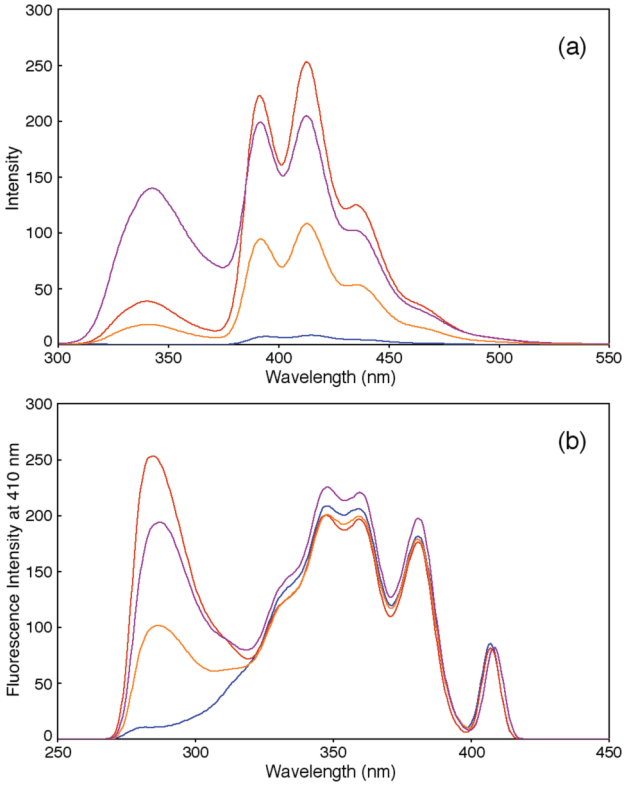

FIGURE 5. (a) Fluorescence emission spectra of free-**4** (blue line), **4@3** (red line), a 1:1:1 mixture of **3**, **4**, and **6** (orange line), and a 1:1:1 mixture of **3**, **4**, and **8** (purple line) upon excitation at 285 nm (1.0×10^{-5} M each in C_6H_6 at 296 K). (b) Fluorescence excitation spectra upon fluorescence emission at 410 nm (1.0×10^{-5} M each in C_6H_6 at 296 K).

Photochemical Stability of 4@3. Figure 6 shows the UV−vis absorption spectral changes of **4@3** and free-**4** in C_6H_6 (2.0×10^{-4} M) at 296 K as a function of irradiation time, upon exposure to air and light (500 W ultra-high-pressure mercury lamp), between 310 and 400 nm centering at 365 nm. The **4** encapsulated in **3** almost remained intact under photoirradiation after 2 h (Figure 6a). In marked contrast, the absorption band of free-**4** in C_6H_6 dramatically decreased under the same photoirradiation conditions (Figure 6b). Figure 7 shows the plots of absorption maxima changes (Abs_{-t}/Abs_{-0}) of **4@3** and free-**4** at 382 nm as a

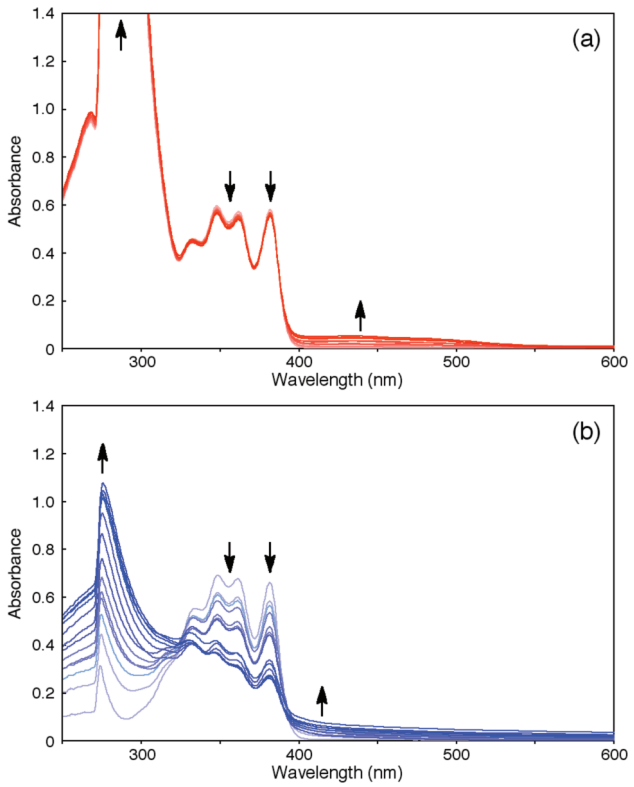

FIGURE 6. UV−vis absorption spectral changes of (a) **4**@**3** and (b) free-**4** (2.0×10^{-4} M in C_6H_6 at 296 K) as a function of irradiation time (10 min each) during the period of 2 h upon exposure to air and light between 310 and 400 nm centering at 365 nm (500 W ultra-high-pressure mercury lamp).

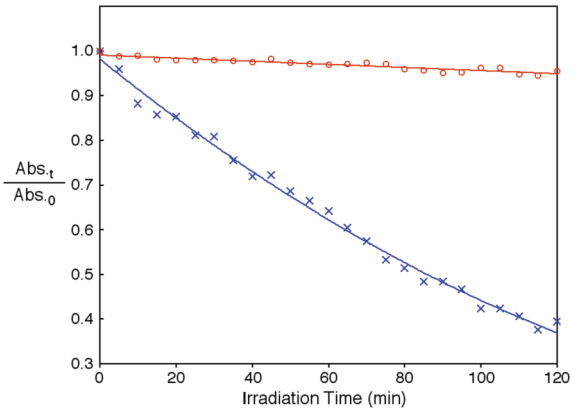

FIGURE 7. Plots of absorption maxima changes (Abs_{-t}/Abs_{-0}) of **4**@**3** (red) and free-**4** (blue) at 382 nm (2.0×10^{-4} M in C_6H_6 at 296 K) as a function of irradiation time upon exposure to air and light (500 W ultra-high-pressure mercury lamp).

function of irradiation time under the same photoirradiation conditions. Figure 8 shows the ^{1}H NMR spectral changes of **4**@**3** and free-**4** in C_6D_6 (1.0×10^{-3} M) at 296 K under the same photoirradiation conditions. After photoirradiation for 1 h, **4**@**3** remained almost intact (Figure 8c), whereas free-**4** dramatically decreased by 87% and new signals appeared (Figure 8g), indicating the formation of photodimers **5** and **5**′ as a result of [4π+4π] photocycloaddition of **4** and 2,6-diacetoxy-9,10-anthraquinone **6** via 9,10-endoperoxide **7** as a result of [4π+2π] photooxygenation of **4** (Figure 1d)

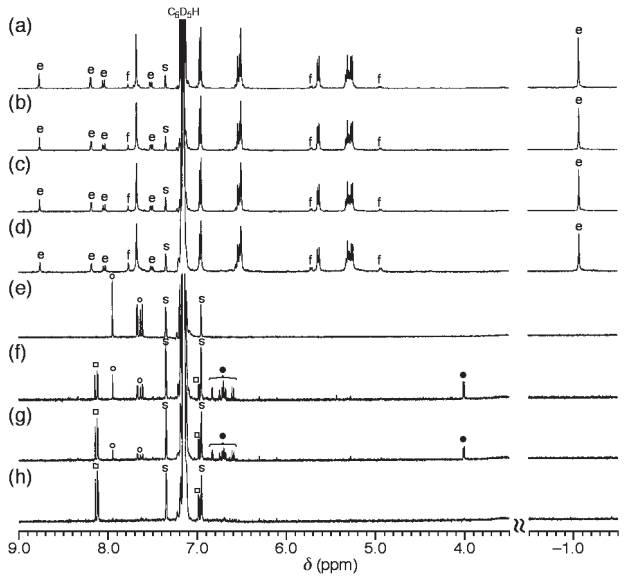

FIGURE 8. Photochemical changes of **4**@**3** and free-**4** (1.0×10^{-3} M in C_6D_6 at 296 K) upon exposure to air and light (500 W ultra-high-pressure mercury lamp), monitored by ^{1}H NMR: photoirradiation of **4**@**3** containing a small amount of free-**3** for (a) 0 h, (b) 0.5 h, (c) 1 h, and (d) 2 h and photoirradiation of free-**4** for (e) 0 h, (f) 0.5 h, (g) 1 h, and (h) 2 h. The signals marked "e" and "f" indicate peaks representing **4** encapsulated in **3** and free-**3**, respectively. The representative signals of free-**4**, photodimers **5** (**5**′), and anthraquinone **6** are marked with open circles, solid circles, and open squares, respectively. The signals marked "s" are the spinning sidebands of the residual solvent (C_6D_5H).

(vide infra). It is noted that **5**, **5**′, and **6** were not produced from **4**@**3** even after 4 h photoirradiation (Figure S5, Supporting Information). Under fluorescent light (room light) and in air the **4**@**3** in C_6D_6 was also stable and remained fully intact for at least 10 days (Figure S6, Supporting Information). These results clearly indicate that the capsule **3** serves as a guard nanocontainer, by its encapsulation of **4**, to protect against the photochemical reactions of **4** (Figure 1b).[13]

At the concentrations used in our experiments, **3** maintains 100% encapsulation of **4** upon addition of 1 equiv of **4**, and **4**@**3** does not release **4**. The capsule **3** can encapsulate only one molecule of **4**, but not two molecules of **4**. Therefore, **3** protects against the formation of photodimers **5** and **5**′ by the encapsulation of **4**. The anthraquinone **6** is formed via 9,10-endoperoxide **7** from **4**. The **4**@**3** possesses four equatorial portals through which singlet oxygen, as the source of the formation of **7**, can come into contact with **4** encapsulated in **3**. However, **7** has a bent molecular shape due to sp^3 carbon atoms at the 9,10-positions. Therefore, **7** and a transition state to reach **7** would not fit the inner cavity of **3** for encapsulation. Thus, **3** protects against the formation of **6** via **7** by the encapsulation of **4**.

In the UV−vis absorption spectra of **4**@**3** under photoirradiation (Figure 6a), the absorption in the region between 400 and 550 nm gradually increased, especially after photoirradiation for 1.5 h. This arises from the decomposition of the linker unit **2** of the capsule **3**, probably due to photooxygenation of the catechol (or catecholate) moiety of the **2** unit to the *o*-semiquinone radical (or *o*-semiquinonate) or *o*-quinone.[16]

(16) (a) Hong, B. H.; Bae, S. C.; Lee, C.-W.; Jeong, S.; Kim, K. S. *Science* **2001**, *294*, 348–351. (b) Sato, O.; Cui, A.; Matsuda, R.; Tao, J.; Hayami, S. *Acc. Chem. Res.* **2007**, *40*, 361–369.

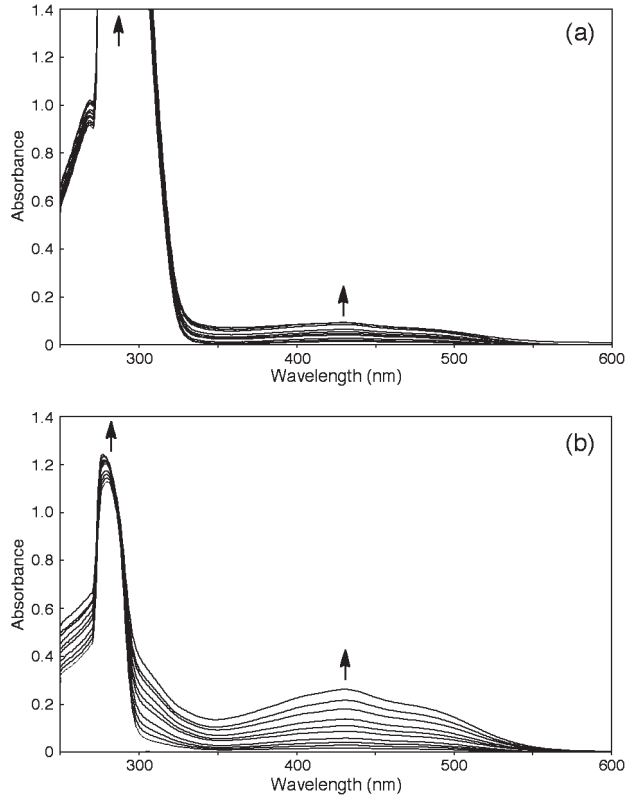

FIGURE 9. UV−vis absorption spectral changes of (a) guest-free **3** and (b) **2** alone (2.0×10^{-4} M in C_6H_6 at 296 K) as a function of irradiation time (10 min each for 2 h in total) upon exposure to air and light (500 W ultra-high-pressure mercury lamp). The concentration of the linker unit **2** of **3** corresponds to 8.0×10^{-4} M because **3** has four molecules of **2** unit.

Figures 9a and 9b show the UV−vis absorption changes of guest-free **3** and **2** alone, respectively, in C_6H_6 at 296 K, as a function of irradiation time upon exposure to air and light (500 W ultra-high-pressure mercury lamp); the colorless solutions gradually became yellow. Photooxygenation of **2** alone was more noticeable than that of free-**3**.

Photochemical Reactions of Free-4. As mentioned above, free-**4** in C_6D_6 (1.0×10^{-3} M) at 296 K is unstable under the photoirradiation conditions used (light and air) (Figure 8e−h). Compound **4** alone in C_6D_6 dramatically changed to a mixture of **4**, **5** (**5**′), and **6** in a 31:35:34 ratio and a 13:28:59 ratio after 0.5 and 1 h of photoirradiation, respectively. After 2 h of photoirradiation, **4** and **5** (**5**′) were fully converted to **6**. During the course of the photoirradiation, 9,10-endoperoxide **7** was not observed. Figure 10 shows the ^{1}H NMR spectra of the photochemical changes of **4** alone under fluorescent light and in air, wherein **7** was observed in addition to **5** (**5**′) and **6**. Free-**4** changed to a mixture of **4**, **5** (**5**′), **6**, and **7** in a 51:19:3:27 ratio and a 36:32:7:25 ratio after 3 days and 5 days of photoirradiation, respectively. Additional photoirradiation led to a decrease in **4** and **7** and an increase in **5** (**5**′) and **6**. The ratio of **4**, **5** (**5**′), **6**, and **7** changed to 11:47:33:9 after 10 days of photoirradiation. The photodimers **5** and **5**′, as regioisomers, were formed in a 51:49 ratio (Figures S9 and S10, Supporting Information).

The stability of the isolated mixture of **5** and **5**′ in C_6D_6 (1.0×10^{-3} M) at 296 K under photoirradiation was also investigated. Under light (500 W ultra-high-pressure mercury lamp) and in air, a mixture of **5** and **5**′ changed to a mixture of **4**, **5** (**5**′), and **6** in a 5:89:6 ratio and a 14:43:43 ratio after 1 and 2 h of photoirradiation, respectively (Figure S7, Supporting Information). After 4 h of photoirradiation, **4** and **5** (**5**′) were fully converted to **6**. This result indicated that **5** and **5**′ reversibly returned to the monomer **4** under this condition and that **6** was formed not directly from **5** but from **4** and **7**. Under fluorescent light and in air, **5** and **5**′ were stable and remained fully intact for at least 10 days (Figure S8, Supporting Information).

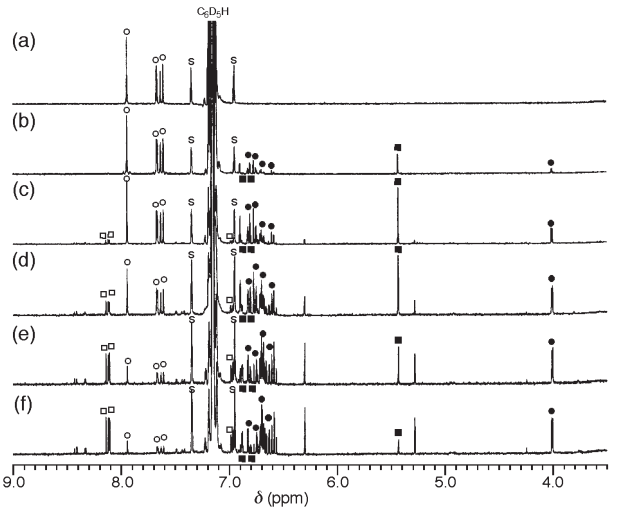

FIGURE 10. ^{1}H NMR spectra for the photochemical changes of free-**4** (1.0×10^{-3} M in C_6D_6 at 296 K) under fluorescent light (room light) and in air: (a) 0 d, (b) 1 d, (c) 3 d, (d) 5 d, (e) 8 d, and (f) 10 d. The representative signals of free-**4**, **5** (**5**′), **6**, and 9,10-endoperoxide **7** are marked with open circles, solid circles, open squares, and solid squares, respectively. The signals marked "s" are the spinning sidebands of the residual solvent (C_6D_5H).

Conclusion

We have found that the self-assembled boronic ester cavitand capsule **3** serves as a photosensitizer for the encapsulated 2,6-diacetoxyanthracene **4** upon excitation at 285 nm, as a result of the energy transfer from the excited **3** to the encapsulated **4**. Upon excitation at 285 nm, the **4** encapsulated in **3** in C_6H_6 showed strong fluorescence emission, while **4** alone in C_6H_6 exhibited very weak emission. We also demonstrated that **3** serves as a guard nanocontainer, by encapsulation of **4**, to protect against the [4π+4π] photodimerization and [4π+2π] photooxygenation of **4**. Compound **4** encapsulated in the capsule **3** in C_6D_6 at 296 K in air is stable upon exposure to an ultra-high-pressure mercury lamp for 4 h and fluorescent light (room light) for 10 days. In marked contrast, free-**4** in C_6D_6 at 296 K in air is unstable under the same photoirradiation conditions; it affords the photodimers **5** and **5**′ and the anthraquinone **6** via 9,10-endoperoxide **7**. The capsule **3** alters the excited-state chemistry of **4** by encapsulating **4** within **3** and suppressing its most favored solution pathway.[9b,d] Thus, the guest-encapsulating capsule **4**@**3** serves as a photostable luminescence material.

A study of the encapsulation and protection of other photoluminescence materials in **3**, such as 2,6-diacetoxy-9,10-bis(phenylethynyl)anthracene, is currently underway in our laboratory.

Experimental Section

General Methods. ^{1}H and ^{13}C NMR spectra were recorded at 400 and 100 MHz, respectively. Photoirradiation was conducted with an ultra-high-pressure mercury lamp (500 W) through a combination of a color filter and a heat-absorbing filter for light between 310 and 400 nm centering at 365 nm. The syntheses of tetrakis(dihydroxyboryl) cavitand **1**, 1,2-bis(3,4-dihydroxyphenyl)-ethane **2**, boronic ester cavitand capsule **3**, and guests **4**, **6**, and **8** have previously been reported.[11] *trans*-1,2-Bis(3,4-dimethoxyphenyl)ethene as a precursor of **2** was also synthesized by the McMurry coupling of 3,4-dimethoxybenzaldehyde according to the literature.[17]

Photodimer 5 and Its Regioisomer 5′. A solution of 2,6-diacetoxyanthracene **4** (40.0 mg, 0.136 mmol) in benzene (136 mL) was stirred at room temperature for 1 h under light (500 W ultra-high-pressure mercury lamp) and in air. After evaporation of solvent, the residue was purified by recycle preparative GPC to give a 51:49 mixture of **5** and **5′** (17.6 mg, 44% yield) as an off-white solid (Figures S9 and S10, Supporting Information) and **6** (20.5 mg, 46% yield) (Figure S11, Supporting Information). **5**: ^{1}H NMR (C_6D_6) δ 6.74 (d, J = 2.0 Hz, 4H), 6.71 (dd, J = 2.0 and 8.3 Hz, 4H), 6.70 (d, J = 8.3 Hz, 4H), 4.02 (s, 4H), 1.69 (s, 12H); ^{1}H NMR ($CDCl_3$) δ 6.89 (d, J = 8.3 Hz, 4H), 6.72 (d, J = 2.4 Hz, 4H), 6.59 (dd, J = 2.4 and 8.3 Hz, 4H), 4.51 (s, 4H), 2.22 (s, 12H). **5′**: ^{1}H NMR (C_6D_6) δ 6.83 (d, J = 2.0 Hz, 4H), 6.68 (dd, J = 2.0 and 8.3 Hz, 4H), 6.59 (d, J = 8.3 Hz, 4H), 4.01 (s, 4H), 1.72 (s, 12H); ^{1}H NMR ($CDCl_3$) δ 6.91 (d, J = 8.3 Hz, 4H), 6.69 (d, J = 2.4 Hz, 4H), 6.58 (dd, J = 2.4 and 8.3 Hz, 4H), 4.51 (s, 4H), 2.21 (s, 12H). **5 and 5′**: ^{13}C NMR ($CDCl_3$) δ 169.28 (169.26), 148.60 (148.52), 144.32 (144.29), 140.14 (140.07), 128.02 (127.80), 120.43 (120.24), 118.44, 52.80 (52.78), 21.12 (21.09).

9,10-Endoperoxide 7. The transformation of 2,6-diacetoxyanthracene **4** (1.0×10^{-3} M) to its 9,10-endoperoxide **7** was carried out in $CDCl_3$ instead of benzene at room temperature under fluorescent light (room light) and in air because this reaction in $CDCl_3$ gave a mixture of **4** and **7** in a 47:53 ratio after 5 days of photoirradiation (Figure S12a, Supporting Information), whereas the reaction in C_6D_6 gave a mixture of **4**, **5** (**5′**), **6**, and **7** even after 3 days of photoirradiation (Figure 10c).

A solution of **4** (30.0 mg, 0.102 mmol) in $CDCl_3$ (10 mL) was stirred at room temperature for 5 days under fluorescent light and in air. At this higher reaction concentration (10×10^{-3} M), the reaction gave a mixture of **4**, **5** (**5′**), and **7** in a 27:2:71 ratio (Figure S13, Supporting Information). After evaporation of solvent, the residue was subjected to recycle preparative GPC to separate **7**, **5** (**5′**), and **4**. However, **7** was decomposed to **6** during the course of this treatment: ^{1}H NMR ($CDCl_3$) δ 7.42 (d, J = 7.8 Hz, 2H), 7.21 (d, J = 2.0 Hz, 2H), 7.02 (dd, J = 2.0 and 7.8 Hz, 2H), 6.02 (s, 2H), 2.31 (s, 6H); ^{1}H NMR (CD_2Cl_2) δ 7.45 (d, J = 7.8 Hz, 2H), 7.21 (d, J = 2.4 Hz, 2H), 7.02 (dd, J = 2.4 and 7.8 Hz, 2H), 6.04 (s, 2H), 2.28 (s, 6H); ^{1}H NMR (C_6D_6) δ 6.90 (d, J = 2.0 Hz, 2H), 6.81 (dd, J = 2.0 and 8.3 Hz, 2H), 6.77 (d, J = 2.0 Hz, 2H), 5.44 (s, 2H), 1.74 (s, 6H); ^{13}C NMR ($CDCl_3$) δ 169.20, 150.11, 139.23, 134.91, 124.83, 120.77, 117.54, 78.61, 21.09.

Acknowledgment. This work was supported in part by a Grant-in-Aid from JSPS (No. 22350060).

Supporting Information Available: Synthetic procedures of **9** and **10** and additional spectral data. This material is available free of charge via the Internet at http://pubs.acs.org.

(17) Shadakshari, U.; Rele, S.; Nayak, S. K.; Chattopadhyay, S. *Indian J. Chem.* **2004**, *43B*, 1934–1938.